



Typing and Species Identification of Clinical *Klebsiella* Isolates by Fourier Transform Infrared Spectroscopy and Matrix-Assisted Laser Desorption Ionization–Time of Flight Mass Spectrometry

Ariane G. Dinkelacker,^{a,b} Sophia Vogt,^{a,b} Philipp Oberhettinger,^{a,b} Norman Mauder,^c Jörg Rau,^d Markus Kostrzewa,^c John W. A. Rossen,^e Ingo B. Autenrieth,^{a,b} Silke Peter,^{a,b}  Jan Liese^{a,b}

^aInstitute of Medical Microbiology and Hygiene, University Hospital Tübingen, Tübingen, Germany

^bGerman Center for Infection Research (DZIF), Partner Site Tübingen, Tübingen, Germany

^cBruker Daltonik GmbH, Bremen, Germany

^dChemisches und Veterinäruntersuchungsamt Stuttgart, Fellbach, Germany

^eUniversity of Groningen, University Medical Center Groningen, Department of Medical Microbiology, Groningen, The Netherlands

ABSTRACT *Klebsiella pneumoniae* and related species are frequent causes of nosocomial infections and outbreaks. Therefore, quick and reliable strain typing is crucial for the detection of transmission routes in the hospital. The aim of this study was to evaluate Fourier transform infrared spectroscopy (FTIR) and matrix-assisted laser desorption ionization–time of flight mass spectrometry (MALDI-TOF MS) as rapid methods for typing clinical *Klebsiella* isolates in comparison to whole-genome sequencing (WGS), which was considered the gold standard for typing and identification. Here, 68 clinical *Klebsiella* strains were analyzed by WGS, FTIR, and MALDI-TOF MS. FTIR showed high discriminatory power in comparison to the WGS reference, whereas MALDI-TOF MS exhibited a low ability to type the isolates. MALDI-TOF mass spectra were further analyzed for peaks that showed high specificity for different *Klebsiella* species. Phylogenetic analysis revealed that the *Klebsiella* isolates comprised three different species: *K. pneumoniae*, *K. variicola*, and *K. quasipneumoniae*. Genome analysis showed that MALDI-TOF MS can be used to distinguish *K. pneumoniae* from *K. variicola* due to shifts of certain mass peaks. The peaks were tentatively identified as three ribosomal proteins (S15p, L28p, L31p) and one stress response protein (YjbJ), which exhibit amino acid differences between the two species. Overall, FTIR has high discriminatory power to recognize the clonal relationship of isolates, thus representing a valuable tool for rapid outbreak analysis and for the detection of transmission events due to fast turnaround times and low costs per sample. Furthermore, specific amino acid substitutions allow the discrimination of *K. pneumoniae* and *K. variicola* by MALDI-TOF MS.

KEYWORDS *Klebsiella pneumoniae*, *Klebsiella variicola*, bacterial typing, Fourier transform infrared spectroscopy, MALDI-TOF mass spectrometry

Rapid and reliable typing of bacterial isolates is a crucial tool for the detection of possible transmission routes of pathogens in the hospital, for the identification of bacterial reservoirs, and for the institution and evaluation of infection control efforts (1, 2). Whereas the discriminatory power of commonly available strain characteristics, such as antimicrobial susceptibility testing (AST) results or biochemical profiles, is usually insufficient to infer clonal relationships between bacterial isolates, DNA-based techniques, such as multilocus sequence typing (MLST), pulsed-field gel electrophoresis

Received 25 May 2018 Returned for modification 22 June 2018 Accepted 19 August 2018

Accepted manuscript posted online 22 August 2018

Citation Dinkelacker AG, Vogt S, Oberhettinger P, Mauder N, Rau J, Kostrzewa M, Rossen JWA, Autenrieth IB, Peter S, Liese J. 2018. Typing and species identification of clinical *Klebsiella* isolates by Fourier transform infrared spectroscopy and matrix-assisted laser desorption ionization–time of flight mass spectrometry. *J Clin Microbiol* 56:e00843-18. <https://doi.org/10.1128/JCM.00843-18>.

Editor Karen C. Carroll, Johns Hopkins University School of Medicine

Copyright © 2018 American Society for Microbiology. All Rights Reserved.

Address correspondence to Jan Liese, jan.liese@med.uni-tuebingen.de.

A.G.D. and S.V. contributed equally to this study.

(PFGE), or repetitive element sequence-based PCR (rep-PCR), have been successfully used for this purpose (3, 4). Advances in DNA sequencing technology have positioned whole-genome sequencing (WGS) as a potential gold standard of future strain typing (5). However, these “high-resolution” techniques are mostly used retrospectively rather than for real-time surveillance, mainly because they are laborious to perform and cost intensive (6).

Fourier transform infrared (FTIR) spectroscopy is a spectrum-based technique that quantifies the absorption of infrared light by molecules present in the sample, such as lipids, nucleic acids, carbohydrates, lipopolysaccharides, and proteins. This results in the generation of a specific FTIR spectrum, which reflects the overall chemical composition of the specimen (7). This technique can be used for bacterial species identification by comparing the spectrum to a reference database. FTIR has also been used for the typing of bacterial isolates such as *Staphylococcus aureus* (8, 9), *Escherichia coli* (10), *Yersinia enterocolitica* (11), *Listeria monocytogenes* (12), and others in samples from human, animal, and environmental sources.

Matrix-assisted laser desorption ionization–time of flight mass spectrometry (MALDI-TOF MS) has become a standard tool for the identification of pathogens in the clinical microbiology laboratory due to easy sample preparation, reliability, and short time to results (13, 14). MALDI-TOF mass spectra resemble specific “fingerprints” of the bacterial species, which are shaped by the masses of abundant proteins present in the bacteria, such as ribosomal proteins. Identification of a strain is then achieved by comparing the spectrum of an unknown isolate to a reference database. However, MALDI-TOF MS can also be successfully employed for strain typing on the basis of distinct protein profiles within a species. This was shown, e.g., for *E. coli* (15) in a specific setting. Diverging results were reported for the typing of *S. aureus* with MALDI-TOF MS. Some groups were able to delineate clonal complexes (16) including methicillin-resistant *S. aureus* strains (17), whereas others reported insufficient discriminatory power of this technique for *S. aureus* as well as for *Enterococcus faecium* (18). In *Campylobacter jejuni*, subgroups could be separated by specific MALDI-TOF spectrum peaks, which represented differences in the amino acid sequence (and therefore mass changes) in certain ribosomal proteins (19). Moreover, this technique can also be used for AST (20), e.g., for rapid detection of resistance to carbapenems and other beta-lactam antibiotics (21, 22).

In this study, we sought to evaluate the discriminatory power of the spectrum-based analysis techniques FTIR spectroscopy and MALDI-TOF MS for strain typing in comparison to whole-genome sequencing (WGS) for potential integration into the routine diagnostic workflow. *Klebsiella pneumoniae* and related species were chosen as test organisms, because they are clinically highly relevant pathogens that can cause severe infections, such as catheter-associated urinary tract infections, bloodstream infections, and sepsis, which often occur in the hospital setting in predisposed patients (e.g., immunocompromised patients and preterm neonates) (23). Moreover, *K. pneumoniae* is a frequent cause of nosocomial outbreaks, which warrant immediate infection control measures, especially if antibiotic-resistant strains are involved (24).

MATERIALS AND METHODS

***Klebsiella* isolates.** A total of 68 isolates, which were collected and analyzed during a 1-year period (December 2013 to November 2014) in the clinical microbiology laboratory of the University Hospital Tübingen, Tübingen, Germany, were used in this study. The strains were recovered from routine microbiological throat and anal swab screening samples that were taken from 57 patients on a neonatal intensive care unit according to German infection control guidelines. The bacterial isolates were stored at -80°C until they were used for WGS, FTIR, and MALDI-TOF analysis.

Genome sequencing and assembly. Genomic DNA was extracted using the UltraClean Microbial DNA isolation kit (Mo Bio Laboratories Inc., Carlsbad, CA, USA). DNA libraries were prepared with the TruSeqNano DNA LT kit or the Nextera XT kit, version 2 (Illumina, San Diego, CA, USA). All libraries were sequenced on an Illumina MiSeq or Illumina Nextseq sequencer (both from Illumina, San Diego, CA, USA). Sequencing reads were assembled using the A5 pipeline (version 20140604) and SPAdes (version 3.7.0) (25, 26).

Genome analysis. Genomic features were annotated using the RAST tool kit (RASTtk) as provided by the online PATRIC genome annotation service, version 3.5.11 (<https://www.patricbrc.org/app/Annotation>). The core genomes of all isolates were generated by Spine (version 0.1.2) (27). Single

nucleotide polymorphisms (SNPs) were called by mapping the high-quality sequencing reads generated by Trimmomatic (28) to the core genome using the BioNumerics software suite, version 7.6 (Applied Maths, Sint-Martens-Latem, Belgium), with strict settings for SNP analysis. Average nucleotide identity (ANI) was calculated using JSpecies based on the ANIm algorithm (29). One representative genome of each WGS cluster was used as the input together with two reference genomes for *K. pneumoniae* (strains 30684/NJST258_2 and HS11286), *Klebsiella variicola* (strains At-22 and GJ1), and *Klebsiella quasipneumoniae* (strains ATCC 700603 and HKUOPA4). Multilocus sequence types (MLST) were extracted from the assembled sequences using the online MLST service for *K. pneumoniae* (version 1.8) provided by the Center for Genomic Epidemiology (<https://cge.cbs.dtu.dk/services/MLST/>) (30).

FTIR spectrum acquisition and analysis. Strains were grown at 37°C without the addition of CO₂ on Columbia sheep blood agar plates (Oxoid, Wesel, Germany) for 18 (±0.5) h before the suspension of a loopful of bacteria in 50 µl of 70% (vol/vol) ethanol in 1.5-ml vials containing sterile metal rods for better homogenization (Bruker Daltonik). After thorough vortexing, 50 µl of sterile H₂O was added. Then 15 µl of the resulting bacterial suspension was placed on a silicon sample plate (Bruker Daltonik), which was dried at 37°C for approximately 20 min. Four technical replicates of all isolates were analyzed in each of three independent experiments on a commercially available IR Biotyper system (Bruker Daltonik) by running the IR Biotyper software (version 1.0.0.73) with the default analysis settings (32 scans per technical replicate; spectral resolution, 6 cm⁻¹; apodization function, Blackman-Harris 3-term; zero-filling factor, 4). Measurements that did not meet the default quality criteria (0.4 < absorption < 2; signal-to-noise ratio, >40; fringes [$\times 10^{-6}$], <100) were excluded from further analysis. Spectrum processing by the software is based on the second derivative of the 800- to 1,300-cm⁻¹ wavenumber range of the spectra, which is the default setting of the manufacturer. After vector normalization, the respective summary spectra were calculated as the average of the underlying (technical or biological) replicate spectra. The similarity of two spectra was assessed as the Euclidean distance (ED) between the two (normalized) corresponding vectors using the following formula: similarity (%) = (1 - ED) × 100. The similarity between all isolate spectra was calculated to generate a matrix, which was subsequently used for clustering the isolates with the average linkage algorithm by the IR Biotyper software. The resulting dendrograms were visualized in BioNumerics, version 7.6.

MALDI-TOF mass spectrum acquisition and analysis. *K. pneumoniae* isolates were grown for 16 to 18 h at 37°C on Columbia sheep blood agar plates (Oxoid). Colony material was directly transferred and spotted onto a reusable 96-spot steel target (Bruker Daltonik, Bremen, Germany). The spots were then overlaid with 1 µl of the matrix solution (α -cyano-4-hydroxycinnamic acid in 50% acetonitrile with 2.5% trifluoroacetic acid) and were air dried for at least 10 min. Each isolate was spotted in four technical replicates in three independent experiments. MALDI-TOF mass spectra for species identification and typing were generated on a MALDI Biotyper system (based on a Microflex LT/SH instrument; Bruker Daltonik) in a mass/charge (*m/z*) range of 2,000 to 20,000 with default settings for routine species identification. The system is calibrated weekly using the IVD Bacterial Test Standard (Bruker Daltonik) as recommended by the manufacturer. Bruker Biotyper software, version 3.1, with the MBT IVD library containing 5,989 mass spectra was used. Measurements not meeting the quality criteria [$\log(\text{score})$, <2.00] were excluded from analysis. Spectrum data were subsequently imported into the BioNumerics software suite, version 7.6. Preprocessing of the spectra (baseline subtraction, smoothing, and noise calculation) was performed using the default settings, before summarizing the spectra of technical and biological replicates, which yielded one summary spectrum per isolate. A curve-based or a peak-based similarity matrix was calculated using the settings for the Pearson correlation or Dice method, respectively, before clustering of the spectra by the software using the Ward algorithm or the unweighted pair group method with arithmetic means (UPGMA).

Peak classes (i.e., consensus mass peaks from several spectra) for interisolate comparison were generated with the standard settings in BioNumerics, version 7.6, except that a threshold of 10% for new classes was used (i.e., a peak had to be present in at least 10% of the spectra to generate a new consensus peak).

Calculation of clustering concordance. After manual attribution of isolates according to the clustering result and application of the desired cluster cutoff value, the adjusted Rand index (ARI) and contingency tables were calculated using the online tool at www.comparingpartitions.info (31).

Ethics statement. The bacterial isolates used in this study were previously collected from routine microbiological specimens and were anonymized. Patients were not physically involved in the current study. According to the professional code of conduct of the Baden-Württemberg Medical Association (Landesärztekammer), approval from an ethics committee is therefore not required.

Accession number(s). The assembled genomes of the *Klebsiella* strains used in this study have been deposited in the European Nucleotide Archive under accession no. PRJEB27975). The following genomes were used as references: *K. pneumoniae* 30684/NJST258_2 (NCBI Reference Sequence Database accession no. NZ_CP006918), *K. pneumoniae* HS11286 (NC_016845), *K. quasipneumoniae* ATCC 700603 (NZ_CP014696), *K. quasipneumoniae* HKUOPA4 (NZ_CP014154), *K. variicola* At-22 (NC_013850), *K. variicola* GJ1 (NZ_CP017284), and *E. coli* K-12 (NC_000913).

RESULTS

***Klebsiella* isolates included in the study.** Weekly microbiological screening specimens (anal and pharyngeal swabs) are routinely taken from patients on the neonatal intensive care units of our hospital as mandated by German infection control guidelines. The first bacterial isolates, which were identified as *K. pneumoniae* by MALDI-TOF

MS at that time, were collected from newly colonized patients born in the 1-year study period (from December 2013 until November 2014). Consecutive isolates were added if a change in the resistance pattern relative to previous isolates from the same patient occurred. Overall, 68 bacterial isolates ("ID 1" through "ID 68") originating from 57 patients were included in this study (see Table S1 in the supplemental material).

SNP-based genome comparison and species identification of *Klebsiella* isolates.

To generate a reference for spectrum-based typing methods, a single nucleotide polymorphism (SNP)-based comparison of all 68 sequenced *Klebsiella* genomes was calculated using a previously built core genome (size, ca. 4.0 Mbp) of all strains (see Materials and Methods for details). Whole-genome sequencing (WGS) allowed for assignment of the strains to 29 WGS clusters (designated "A" through "CC" [Fig. 1]), where two isolates exhibiting a difference of <18 SNPs (32) were considered to belong to the same cluster. Eighteen WGS clusters contained only a single isolate, whereas 11 clusters comprised 2 to 8 isolates (Fig. 1). Comparison of the multilocus sequence types (MLST) (which were extracted from WGS data) of clusters with a genomic distance of <600 SNPs revealed that both clusters A and B (123-SNP distance) belonged to ST14, whereas clusters E and F (362-SNP distance), as well as clusters W and X (555-SNP distance), belonged to different sequence types (ST540, ST1013, ST922, and ST704, respectively) (Fig. 1). Taking these findings together, the strain distribution reflects a great diversity of *Klebsiella* strains recovered from our neonatal intensive care unit and is therefore ideally suited for determining the resolution of typing techniques.

The SNP-based dendrogram further suggested that WGS clusters could be assigned to three clades (designated clades I, II, and III) based on greater SNP distances (Fig. 1): clade I contained 24 clusters (A through X; 53 isolates); clade II consisted solely of cluster Y (4 isolates); and clade III comprised 4 WGS clusters (Z through CC; 11 isolates). Earlier versions of MALDI-TOF MS databases used for bacterial identification were not able to consistently separate the species *K. pneumoniae*, *K. variicola*, and *K. quasipneumoniae*, which can result in misidentification (33). Therefore, we calculated the average nucleotide identity (ANI) between one representative isolate of each WGS cluster (Fig. 1) and two reference genomes for each of the three *Klebsiella* species, because ANI values of >95% indicate classification as the same species (29). All clade I isolates showed an ANI of >95% relative to *K. pneumoniae* reference isolates, whereas the clade II and III isolates exhibited ANI of >96% relative to the *K. quasipneumoniae* and *K. variicola* references, respectively (see Table S2 in the supplemental material). This confirms that *Klebsiella* species identification by MALDI-TOF MS is highly dependent on the database. From here on, the species attribution of the isolates used in this study is derived from the ANI calculations.

FTIR spectroscopy-based typing. FTIR is a rapid and easy-to-perform approach for the analysis of bacterial cultures. We used this technique to analyze the heterogeneous collection of 68 *Klebsiella* isolates by acquiring infrared spectra for each isolate in quadruplicate in three independent measurements. The four spectra from one measurement (technical replicates) were summarized by averaging to reduce spectrum noise. These biological replicates were then again summarized to yield an isolate summary spectrum, which was used for further calculations. The similarity between two spectra is assessed by calculating the Euclidean distance between their normalized vectors and is reflected by the distance of the two spectrum curves (see Fig. S1 in the supplemental material). Identical spectra have a similarity of 100%. To determine the intraexperimental variation, the average similarity of the four technical replicates was calculated for each isolate in each experiment. This resulted in a mean similarity of 93.8% with a standard deviation (SD) of $\pm 2.4\%$. Accordingly, the interexperimental variation was calculated from the three biological replicate spectra for each isolate and resulted in a similarity of $88.6\% \pm 4.0\%$ (mean \pm SD). Certain regions of the normalized absorbance spectrum exhibited great variability when all isolate spectra were compared (Fig. S1). This might imply that certain wavenumber ranges (e.g., 1,020 to 1,080 cm^{-1}) play a greater role than others (e.g., 840 to 880 cm^{-1}) in the discrimination of two isolates.

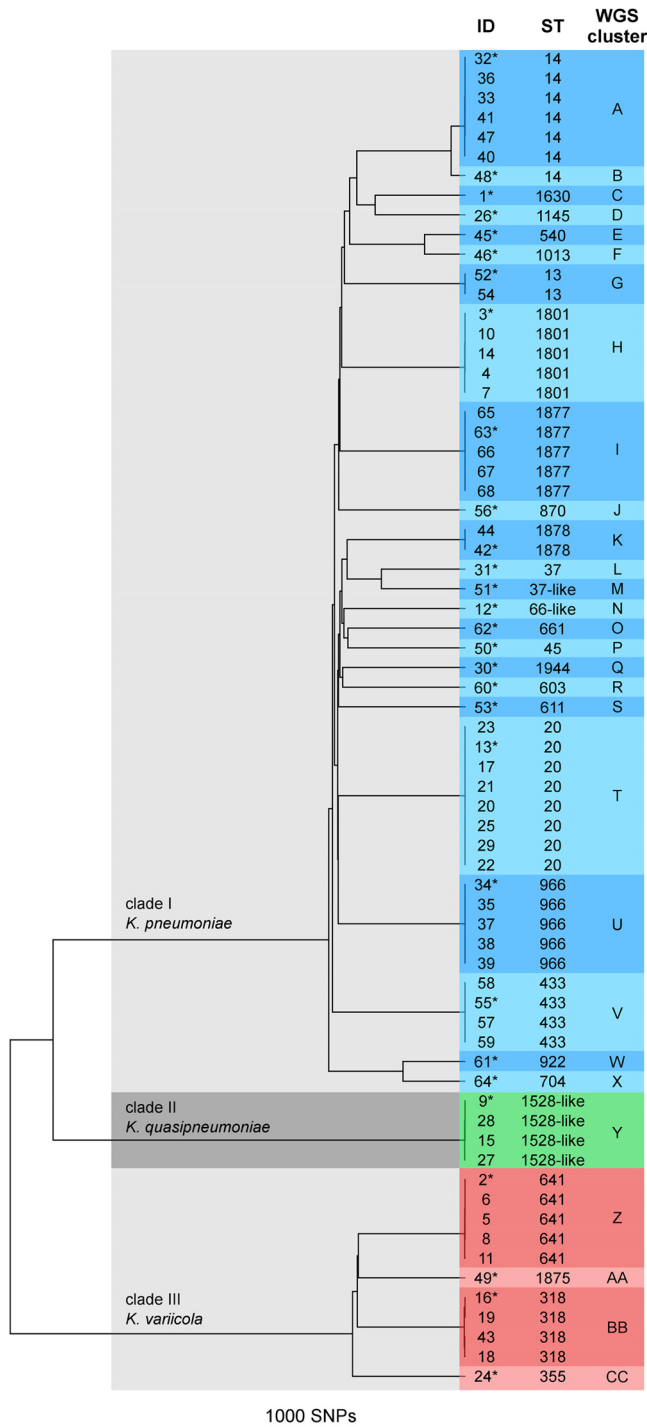


FIG 1 SNP-based cluster dendrogram of 68 *Klebsiella* isolates. A core genome of all genome sequences was used to call SNPs in the isolate genomes. Genomes with distances of <18 SNPs were assigned to the same WGS cluster (colored boxes). The multilocus sequence type (ST) was extracted from the assembled genome sequences. Clade assignment and species identification were derived from average nucleotide identity analysis (Table S2 in the supplemental material) of one representative isolate (indicated by an asterisk) from each cluster.

Calculation of the Euclidean distance between all summary (isolate) spectra and subsequent clustering with the average linkage algorithm resulted in the dendrogram shown in Fig. 2A. To define a suitable cutoff for cluster designation, we reasoned that FTIR spectra of genetically similar isolates will exhibit high similarity, whereas the

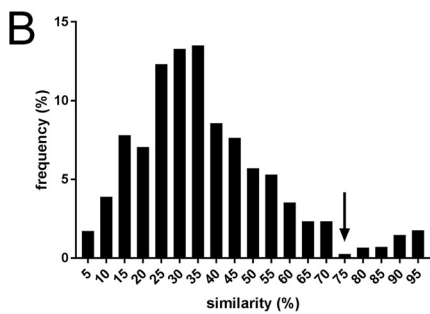
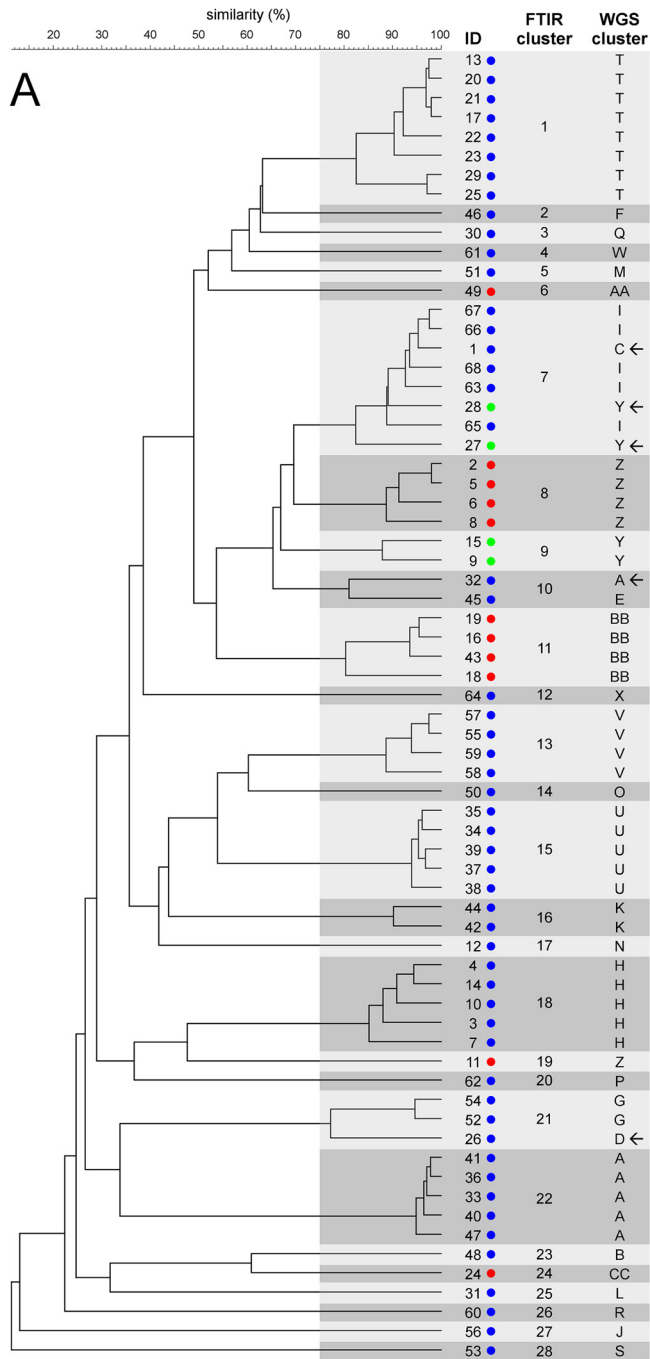


FIG 2 Clustering of FTIR spectra of 68 *Klebsiella* isolates. (A) The dendrogram was calculated by UPGMA clustering of the pairwise Euclidean distances of the isolate spectra. Clusters are displayed as shaded

(Continued on next page)

similarity of distinct isolates will be lower. Indeed, when the similarity values of all possible 2,278 isolate pairs were plotted in a histogram, a bimodal distribution was observed (Fig. 2B). Seventy-five percent similarity was chosen as a cutoff value for clustering, since this value showed the least frequency between the two distribution peaks. When this value was applied to the dendrogram, the 68 isolates were grouped into 28 clusters (designated FTIR clusters 1 through 28 [Fig. 2A]), which comprised one to eight isolates. The adjusted Rand index (ARI) can be used to quantify the congruence of the resulting cluster composition (31). An ARI of 1.0 signals complete concordance between two typing methods. Clustering by WGS analysis and FTIR typing gave highly similar results in our study, which was reflected by an ARI of 0.837. A result congruent with the WGS phylogeny was obtained for 63 (92.6%) isolates. Only 5 isolates (7.4%) showed incongruent results (Fig. 2A), as follows. ID 32 was separated from the other isolates belonging to WGS cluster A and was joined with ID 45 (WGS cluster E) to form FTIR cluster 10. ID 27 and ID 28 were separated from other isolates belonging to WGS cluster Y and were joined with isolates from WGS cluster I to form FTIR cluster 7. This FTIR cluster also contained ID 1, which is the sole member of WGS cluster C. ID 26 (WGS cluster D) was joined with ID 54 and ID 52 (both from WGS cluster G) in FTIR cluster 21. In all other cases, the members of WGS and FTIR clusters were congruent. Interestingly, one isolate (ID 48, in WGS cluster B) that showed a distance of only 123 SNPs from isolates in WGS cluster A was also clearly separated from those isolates by FTIR typing.

These results show that the relatedness of *Klebsiella* strains can be rapidly assessed by FTIR spectroscopy with high resolution that exhibits high congruency with phylogenetic analysis of whole-genome sequencing data and also with multilocus sequence types.

Typing of *Klebsiella* isolates by MALDI-TOF MS. Having established a WGS-based typing reference, we also determined whether MALDI-TOF MS can provide a rapid tool for analyzing the heterogeneous set of *Klebsiella* isolates. The MALDI-TOF spectra of all isolates were recorded in quadruplicate (“technical replicates”). These four spectra were then used to calculate a summary spectrum (“biological replicate”). Three of these biological replicates were acquired for each isolate on three different days and were again summarized to yield the isolate spectrum (see Fig. S2 in the supplemental material). Initially, the similarity between all isolate spectra was quantified by the Pearson coefficient for the spectrum curve, which resulted in the dendrogram shown in Fig. 3A. The UPGMA algorithm was used for clustering, and a similarity cutoff value was chosen that led to the generation of the same number of clusters (29 clusters) as the WGS reference. The ARI was then calculated to quantify the congruency (i.e., the similarity of the composition of the resulting clusters) between MALDI-TOF MS typing and the WGS reference. The chosen parameters resulted in an ARI of 0.356, which indicated a low ability of MALDI-TOF MS to identify related isolates. Isolates belonging to the same WGS cluster (e.g., cluster A) were often assigned to more than one MALDI-TOF cluster, and isolates from distinct WGS clusters (e.g., clusters P and D) were grouped into one MALDI-TOF cluster (see Table S3 in the supplemental material).

Since the clustering of the MALDI-TOF spectra is influenced by the choice of the method of spectrum similarity calculation, by the clustering algorithm, and by the cluster cutoff value, different combinations of algorithms and parameters were used to determine if the ARI could be substantially improved in this way. However, comparison of two spectrum similarity calculation methods (curve-based Pearson similarity and peak-based Dice similarity), two different clustering algorithms (UPGMA and Ward’s algorithm), and different clustering cutoff values, resulting in a wide range of cluster

FIG 2 Legend (Continued)

boxes. The species of each isolate is indicated by a colored circle (blue, *K. pneumoniae*; red, *K. variicola*; green, *K. quasipneumoniae*), and the corresponding WGS cluster of the isolate is derived from Fig. 1. Incongruently clustered isolates are marked with arrows. (B) Frequency distribution of all pairwise FTIR spectrum similarities. The similarity value with the lowest frequency (arrow) between the peaks of the bimodal distribution was used as the cluster cutoff in panel A.

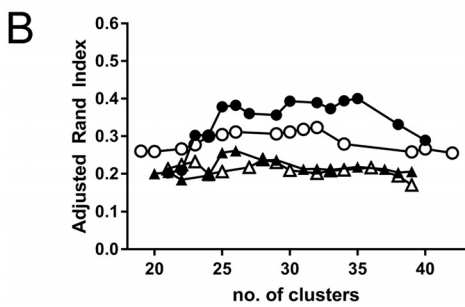
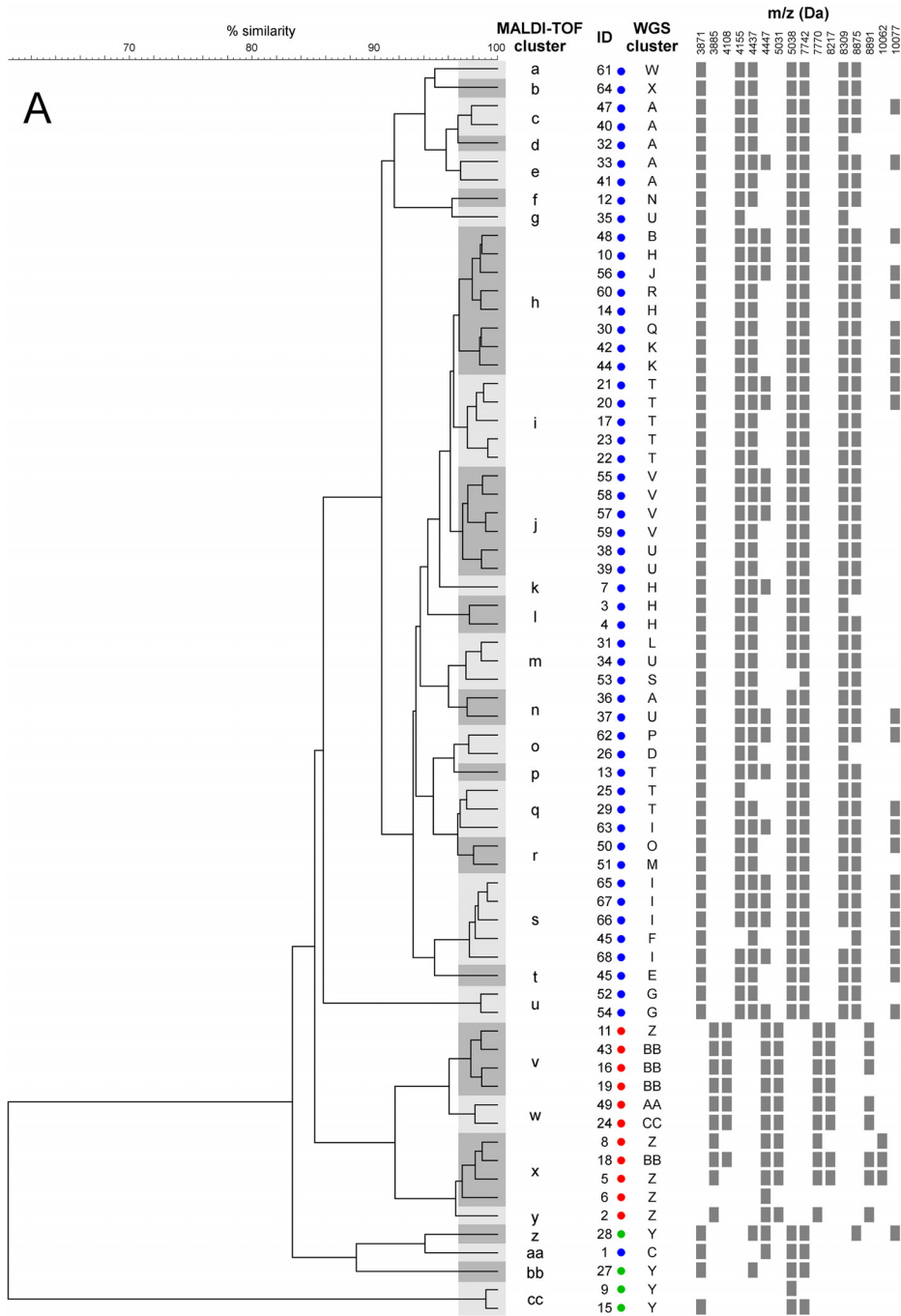


FIG 3 Clustering of MALDI-TOF spectra of 68 *Klebsiella* isolates. (A) UPGMA clustering resulted in 29 MALDI-TOF clusters (shaded boxes). The species of each isolate is indicated by a colored circle (blue, *K. pneumoniae*; red, (Continued on next page)

numbers, showed that even optimization of the calculation parameters can increase the ARI only marginally, to 0.400 (Fig. 3B). These results show that MALDI-TOF MS does not provide the required resolution for typing a diverse set of *Klebsiella* species.

Molecular basis of identification of *K. pneumoniae* and *K. variicola* by MALDI-TOF MS. Although MALDI-TOF MS was only poorly able to assess the relationships of *Klebsiella* isolates, the spectrum-based dendrogram suggested that *K. variicola* isolates could be distinguished from *K. pneumoniae* strains, because the isolate spectra of the respective species clustered together (Fig. 3A). We reasoned that specific MALDI-TOF spectrum peaks within the complete spectrum can provide a basis for the distinction of the two species.

In a first step, the BioNumerics software was used to search for MALDI-TOF mass peaks that were specific for either the *K. pneumoniae* or the *K. variicola* species. This resulted in the identification of 8 candidate peak pairs with similar m/z positions that occurred in either of the two species isolates (Fig. 3A). These mass peaks likely represent the same protein with one or more variations in the amino acid sequence, which alter the molecular mass. Furthermore, some mass peaks exhibited an m/z ratio approximately half that of other peaks. These two peaks likely represent the singly (z) and doubly ($2z$) charged ions of the same protein. These considerations together suggested that four specific proteins with distinct amino acid sequences in *K. pneumoniae* and *K. variicola* can be detected using MALDI-TOF MS.

Many bacterial MALDI-TOF mass spectrum peaks represent ribosomal proteins. To provide a molecular explanation for the observed mass peak shifts, the amino acid sequences of all ribosomal proteins were extracted from the annotated genomes of *K. pneumoniae* and *K. variicola* reference strains as well as from two representative isolates (ID 1 and ID 2), and the molecular masses of the proteins were calculated (see Table S4 in the supplemental material). The removal of the leading methionine from the peptide is a posttranslational modification that occurs in some ribosomal proteins (34). Therefore, the theoretical m/z position for each protein was also calculated for the demethionated form and for the corresponding doubly charged ($2z$) ions. Three ribosomal proteins (L31p, L28p, and S15p) could be identified whose molecular masses matched those of the tentative MALDI-TOF mass peaks (Fig. 4; also Table S4). The different peak positions in the MALDI-TOF spectra of *K. pneumoniae* and *K. variicola* strains could therefore likely be explained by amino acid substitutions in ribosomal proteins (Table 1).

One prominent specific MALDI-TOF mass peak did not correspond to a ribosomal protein based on comparison of the molecular masses. Therefore, the annotated genomes of one *K. pneumoniae* (ID 1) and one *K. variicola* (ID 2) isolate were searched for gene products with molecular masses of ca. 8,309 Da and 8,217 Da, respectively. Indeed, one protein (YjbJ) could be identified whose calculated mass matched the tentative peak masses in the two isolates (Fig. 4; see also Table S5 in the supplemental material). Two amino acid sequence substitutions were responsible for the observed mass difference (Fig. 4 and Table 1). Interestingly, YjbJ is a putative stress response family protein, which was also found in MALDI-TOF mass spectra in *E. coli* (35). It seems very likely that the species-specific MALDI-TOF mass peak also represents the YjbJ protein in *Klebsiella* species.

Overall, these results show that *K. pneumoniae* and *K. variicola* can be distinguished by MALDI-TOF MS using specific mass peaks, which likely represent three ribosomal proteins and one putative stress response protein that exhibit different amino acid sequences in the two species.

FIG 3 Legend (Continued)

K. variicola; green, *K. quasipneumoniae*). The corresponding WGS cluster of the isolate is derived from Fig. 1. The presence of a specific MALDI-TOF mass peak in an isolate spectrum is shown by a filled rectangle in the column under the respective m/z ratio. (B) Differences in the adjusted Rand index among two spectrum similarity calculation algorithms (the curve-based Pearson coefficient [circles] and peak-based Dice algorithm [triangles]) and two clustering algorithms (UPGMA [filled symbols] and Ward's algorithm [open symbols]) with different numbers of clusters.

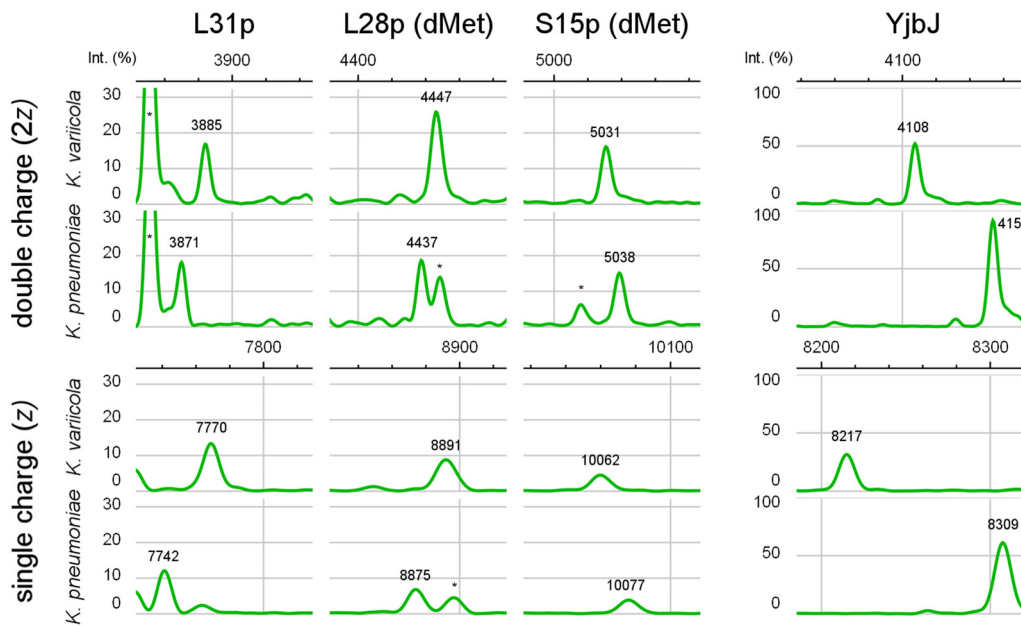


FIG 4 Species-specific MALDI-TOF mass peaks. Shown are MALDI-TOF spectrum peaks for *K. pneumoniae* (ID 32) and *K. variicola* (ID 49) that represent the singly (*z*) or doubly (*2z*) charged ions of three ribosomal proteins (unmodified or with the leading methionine removed [dMet]) and one stress response protein. The *m/z* ratios of the peaks are given. The height of each peak reflects the relative intensity (Int.) with respect to the highest peak in the spectrum. Neighboring peaks without relevance for the species delineation are marked by asterisks.

DISCUSSION

In the study presented here, the performance of FTIR and MALDI-TOF MS for typing clinical *Klebsiella* isolates was evaluated with regard to the discriminatory power of these rapid analysis methods. WGS was employed as a reference to analyze a set of *Klebsiella* strains recovered from clinical specimens. The adjusted Rand index was used to determine the congruency of the respective spectrum-based typing method in comparison to the reference (31).

High agreement between FTIR- and WGS-based clustering was obtained in our study. This is in line with reports that found good discrimination of other clinically or environmentally relevant Gram-negative organisms, such as *Y. enterocolitica* (11, 36), *E. coli* (10), and *Klebsiella oxytoca* (37). These findings might reflect the fact that FTIR spectra are prominently shaped by components of the Gram-negative cell wall or capsule molecules and that high diversity among these structures (e.g., O antigens or capsule types) underlies successful discrimination by FTIR. This hypothesis can be transferred to our study, because nine O serotypes (38) and at least 134 capsule synthesis loci (39) have been described for *K. pneumoniae*. Since clustering by FTIR

TABLE 1 Amino acid sequences of ribosomal and stress response proteins tentatively underlying the species-specific MALDI-TOF spectrum peaks in *K. pneumoniae* and *K. variicola*^a

Protein	Species	Amino acid sequence ^b	Modification	<i>m/z</i>	<i>m/(2z)</i>
L31p	<i>K. pneumoniae</i>	MKKGIHPN <u>Y</u> DEITATCSCGNVMKIRSTVGHDLNLDV[...]*		7,742	3,871
	<i>K. variicola</i>	MKKGIHPK <u>Y</u> EEITATCSCGNVMKIRSTVGHDLNLDV[...]*		7,770	3,885
L28p	<i>K. pneumoniae</i>	(M)SRVCQ[...] <u>J</u> VSAKGMRVIDKKGIDTVL <u>S</u> ELRARGEKY*	dMet	8,875	4,437
	<i>K. variicola</i>	(M)SRVCQ[...] <u>J</u> VSAKGMRVIDKKGIDTVL <u>S</u> ELRARGEKY*	dMet	8,891	4,446
S15p	<i>K. pneumoniae</i>	(M)SLSVE[...] <u>J</u> QRRKLLDYLKRKDVARY <u>A</u> ALIERLGLRR*	dMet	10,077	5,038
	<i>K. variicola</i>	(M)SLSVE[...] <u>J</u> QRRKLLDYLKRKDVARY <u>S</u> ALIERLGLRR*	dMet	10,062	5,031
YjbJ	<i>K. pneumoniae</i>	MNKDEIGGNW <u>K</u> Q <u>E</u> KG[...] <u>J</u> YEKDQAEKEVSDWEHKNDYRW*		8,309	4,155
	<i>K. variicola</i>	MNKDEIGGNW <u>K</u> Q <u>L</u> KG[...] <u>J</u> YAKDQAEKEVSDWEHKNDYRW*		8,217	4,108

^aThe calculated molecular mass was used to determine the theoretical peak position of the single (*m/z*) or double [*m/(2z)*] charged ion of the unmodified or demethionated (dMet) form of the protein.

^bAmino acid substitutions that lead to a mass change are underlined. Ellipses within brackets indicate parts of the sequence without differences; asterisks indicate stop codons.

differed from cluster assignment by WGS for five isolates (7.4%) in this study, we speculate that structural similarities of cell wall or capsule components between isolates are, at least in some cases, responsible for the wrong attribution. As with other DNA-based and non-DNA-based typing techniques, caution has to be used in the interpretation of typing results, especially in the clinical setting.

Since FTIR spectra represent the chemical composition of a specimen, one concern with this technique is that growth of bacteria on different culture media or for different incubation periods will result in changes in the recorded isolate spectra, thereby disturbing reproducibility. This can have a considerable influence on the grouping of isolates, if spectra from the same isolate show substantial dissimilarities. Even the spectra of technical replicates exhibit a certain amount of dissimilarity, which is usually <0.1 of the Euclidean distance. Therefore, it is crucial to keep the growth conditions as constant as possible when one is performing FTIR.

In contrast to FTIR, low congruency between MALDI-TOF MS and WGS typing was found in this study. However, the clustering algorithm that is applied to the similarity matrix, as well as the choice of a cutoff similarity value for clustering, naturally can have an influence on the concordance with the reference. Therefore, two spectrum similarity calculation methods (Pearson and Dice), as well as two clustering algorithms (UPGMA and Ward) and several clustering cutoff values, were evaluated, but even optimization of these parameters could not substantially enhance the performance of MALDI-TOF MS for typing. These results can be explained by the limited intraspecies variation of the protein profile (consisting of ribosomal and other abundant proteins) detected by this method. The highly distinct capacities of FTIR and MALDI-TOF MS to delineate *Klebsiella* isolates support the notion that the "target structures" of the two methods are fundamentally different. Our findings are in line with a recent study that analyzed 83 *K. pneumoniae* isolates representing major multidrug-resistant clones from southern Europe and found low agreement between MALDI-TOF MS and other methods (40).

Nevertheless, we identified 8 MALDI-TOF mass peaks that could be used for the delineation of the two species *K. pneumoniae* and *K. variicola*. This approach has also been successfully employed for the typing of *C. jejuni*, where mass shifts of a specific peak could be attributed to certain multilocus sequence types (19). In a large outbreak with Shiga toxin-positive *E. coli* O104:H4 in Germany, the outbreak strain could also be detected by MALDI-TOF MS by a specific mass peak (41). Also in *E. coli*, a peak shift from 9,741 Da to 9,716 Da showed accurate discrimination for identification of the B2 phylogroup (42). This peak most likely represents the stress response protein HdeA (43, 44). When we used the WGS data from our strains and from available reference genomes, we determined that the tentative peak mass shifts in *K. pneumoniae* and *K. variicola* can be explained by differences in the amino acid sequences of three ribosomal proteins (L31p, L28p, and S15p) and one putative stress response protein (YjbJ). This provides a molecular basis for the way in which closely related species, subspecies, and subtypes can be distinguished by MALDI-TOF MS. However, definitive assignment of MALDI-TOF mass peaks to certain proteins or biomarkers would require additional methods, such as MALDI-TOF tandem MS (MS-MS). With the increased availability of genome sequencing and proteomics technology, it seems desirable to identify more of these type-specific targets, which can be used in MALDI-TOF MS analyses. For example, in *K. pneumoniae*, the presence of an 11,109-Da mass peak was associated with carbapenemase-producing isolates (45–47). Our study included only one strain (four isolates) of *K. quasipneumoniae*, so further investigations with a larger set of strains are needed to determine if this species can also be reliably delineated by MALDI-TOF MS.

Currently, most clinical epidemiological studies and outbreak reports focus on antibiotic-resistant pathogens. However, the spread of antibiotic-susceptible bacteria is often overlooked, despite the fact that these pathogens can also pose a severe threat to immunocompromised patients and other groups who are highly susceptible to infection. Detection of the clonal relationships of pathogens by rapid typing techniques can have a great impact on infection control measures in the hospital.

Overall, our study shows that FTIR is a powerful tool for the typing of *Klebsiella* isolates. Major advantages over WGS include (i) low cost, (ii) little hands-on time, (iii) a fast turnaround time in the laboratory, and (iv) relatively low computation power. These characteristics might allow this technology to be applied for personalized real-time surveillance of pathogenic *Klebsiella* isolates, and potentially other clinically relevant pathogens, independently of their antibiotic susceptibility patterns. However, prospective studies are needed to show feasibility in the laboratory and an impact on patient outcomes.

SUPPLEMENTAL MATERIAL

Supplemental material for this article may be found at <https://doi.org/10.1128/JCM.00843-18>.

SUPPLEMENTAL FILE 1, PDF file, 1.2 MB.

ACKNOWLEDGMENTS

N.M. and M.K. are employees of Bruker Daltonik GmbH, the manufacturer of the MALDI Biotyper and IR Biotyper systems.

REFERENCES

- Li W, Raoult D, Fournier PE. 2009. Bacterial strain typing in the genomic era. *FEMS Microbiol Rev* 33:892–916. <https://doi.org/10.1111/j.1574-6976.2009.00182.x>.
- van Belkum A, Tassios PT, Dijkshoorn L, Haeggman S, Cookson B, Fry NK, Fussing V, Green J, Feil E, Gerner-Smidt P, Brisse S, Struelens M; ESCMID Study Group on Epidemiological Markers. 2007. Guidelines for the validation and application of typing methods for use in bacterial epidemiology. *Clin Microbiol Infect* 13(Suppl 3):S1–S46. <https://doi.org/10.1111/j.1469-0691.2007.01732.x>.
- Sabat AJ, Budimir A, Nashev D, Sa-Leao R, van Dijl J, Laurent F, Grundmann H, Friedrich AW; ESCMID Study Group on Epidemiological Markers. 2013. Overview of molecular typing methods for outbreak detection and epidemiological surveillance. *Euro Surveill* 18:20380. <https://doi.org/10.2807/ese.18.04.20380-en>.
- Deurenberg RH, Bathoorn E, Chlebowicz MA, Couto N, Ferdous M, Garcia-Cobos S, Kooistra-Smid AM, Raangs EC, Rosema S, Veloo AC, Zhou K, Friedrich AW, Rossen JW. 2017. Application of next generation sequencing in clinical microbiology and infection prevention. *J Biotechnol* 243:16–24. <https://doi.org/10.1016/j.jbiotec.2016.12.022>.
- Bertelli C, Greub G. 2013. Rapid bacterial genome sequencing: methods and applications in clinical microbiology. *Clin Microbiol Infect* 19: 803–813. <https://doi.org/10.1111/1469-0691.12217>.
- Rossen JWA, Friedrich AW, Moran-Gilad J. 2018. Practical issues in implementing whole-genome-sequencing in routine diagnostic microbiology. *Clin Microbiol Infect* 24:355–360. <https://doi.org/10.1016/j.cmi.2017.11.001>.
- Wenning M, Scherer S. 2013. Identification of microorganisms by FTIR spectroscopy: perspectives and limitations of the method. *Appl Microbiol Biotechnol* 97:7111–7120. <https://doi.org/10.1007/s00253-013-5087-3>.
- Johler S, Stephan R, Althaus D, Ehling-Schulz M, Grunert T. 2016. High-resolution subtyping of *Staphylococcus aureus* strains by means of Fourier-transform infrared spectroscopy. *Syst Appl Microbiol* 39: 189–194. <https://doi.org/10.1016/j.syapm.2016.03.003>.
- Fetsch A, Contzen M, Hartelt K, Kleiser A, Maassen S, Rau J, Kraushaar B, Layer F, Strommenger B. 2014. *Staphylococcus aureus* food-poisoning outbreak associated with the consumption of ice-cream. *Int J Food Microbiol* 187:1–6. <https://doi.org/10.1016/j.ijfoodmicro.2014.06.017>.
- Sousa C, Novais A, Magalhaes A, Lopes J, Peixe L. 2013. Diverse high-risk B2 and D *Escherichia coli* clones depicted by Fourier transform infrared spectroscopy. *Sci Rep* 3:3278. <https://doi.org/10.1038/srep03278>.
- Kuhm AE, Suter D, Felleisen R, Rau J. 2009. Identification of *Yersinia enterocolitica* at the species and subspecies levels by Fourier transform infrared spectroscopy. *Appl Environ Microbiol* 75:5809–5813. <https://doi.org/10.1128/AEM.00206-09>.
- Davis R, Mauer LJ. 2011. Subtyping of *Listeria monocytogenes* at the haplotype level by Fourier transform infrared (FT-IR) spectroscopy and multivariate statistical analysis. *Int J Food Microbiol* 150:140–149. <https://doi.org/10.1016/j.ijfoodmicro.2011.07.024>.
- Croxatto A, Prod'homme G, Greub G. 2012. Applications of MALDI-TOF mass spectrometry in clinical diagnostic microbiology. *FEMS Microbiol Rev* 36:380–407. <https://doi.org/10.1111/j.1574-6976.2011.00298.x>.
- Clark AE, Kaleta EJ, Arora A, Wolk DM. 2013. Matrix-assisted laser desorption ionization–time of flight mass spectrometry: a fundamental shift in the routine practice of clinical microbiology. *Clin Microbiol Rev* 26:547–603. <https://doi.org/10.1128/CMR.00072-12>.
- Siegrist TJ, Anderson PD, Huen WH, Kleinheinz GT, McDermott CM, Sandrin TR. 2007. Discrimination and characterization of environmental strains of *Escherichia coli* by matrix-assisted laser desorption/ionization time-of-flight mass spectrometry (MALDI-TOF-MS). *J Microbiol Methods* 68:554–562. <https://doi.org/10.1016/j.mimet.2006.10.012>.
- Josten M, Reif M, Szekat C, Al-Sabti N, Roemer T, Sparbier K, Kostrzewa M, Rohde H, Sahl HG, Bierbaum G. 2013. Analysis of the matrix-assisted laser desorption ionization–time of flight mass spectrum of *Staphylococcus aureus* identifies mutations that allow differentiation of the main clonal lineages. *J Clin Microbiol* 51:1809–1817. <https://doi.org/10.1128/JCM.00518-13>.
- Wolters M, Rohde H, Maier T, Belmar-Campos C, Franke G, Scherpe S, Aepfelbacher M, Christner M. 2011. MALDI-TOF MS fingerprinting allows for discrimination of major methicillin-resistant *Staphylococcus aureus* lineages. *Int J Med Microbiol* 301:64–68. <https://doi.org/10.1016/j.ijmm.2010.06.002>.
- Lasch P, Fleige C, Stammler M, Layer F, Nubel U, Witte W, Werner G. 2014. Insufficient discriminatory power of MALDI-TOF mass spectrometry for typing of *Enterococcus faecium* and *Staphylococcus aureus* isolates. *J Microbiol Methods* 100:58–69. <https://doi.org/10.1016/j.mimet.2014.02.015>.
- Zautner AE, Masanta WO, Tareen AM, Weig M, Lugert R, Gross U, Bader O. 2013. Discrimination of multilocus sequence typing-based *Campylobacter jejuni* subgroups by MALDI-TOF mass spectrometry. *BMC Microbiol* 13:247. <https://doi.org/10.1186/1471-2180-13-247>.
- Kostrzewa M, Sparbier K, Maier T, Schubert S. 2013. MALDI-TOF MS: an upcoming tool for rapid detection of antibiotic resistance in microorganisms. *Proteomics Clin Appl* 7:767–778. <https://doi.org/10.1002/prca.201300042>.
- Burckhardt I, Zimmermann S. 2011. Using matrix-assisted laser desorption ionization–time of flight mass spectrometry to detect carbapenem resistance within 1 to 2.5 hours. *J Clin Microbiol* 49:3321–3324. <https://doi.org/10.1128/JCM.00287-11>.
- Jung JS, Popp C, Sparbier K, Lange C, Kostrzewa M, Schubert S. 2014. Evaluation of matrix-assisted laser desorption ionization–time of flight mass spectrometry for rapid detection of beta-lactam resistance in Enterobacteriaceae derived from blood cultures. *J Clin Microbiol* 52: 924–930. <https://doi.org/10.1128/JCM.02691-13>.
- Podschun R, Ullmann U. 1998. *Klebsiella* spp. as nosocomial pathogens:

- epidemiology, taxonomy, typing methods, and pathogenicity factors. *Clin Microbiol Rev* 11:589–603.
24. Campos AC, Albiero J, Ecker AB, Kuroda CM, Meirelles LE, Polato A, Tognim MC, Wingeter MA, Teixeira JJ. 2016. Outbreak of *Klebsiella pneumoniae* carbapenemase-producing *K pneumoniae*: a systematic review. *Am J Infect Control* 44:1374–1380. <https://doi.org/10.1016/j.ajic.2016.03.022>.
 25. Coil D, Jospin G, Darling AE. 2015. A5-miseq: an updated pipeline to assemble microbial genomes from Illumina MiSeq data. *Bioinformatics* 31:587–589. <https://doi.org/10.1093/bioinformatics/btu661>.
 26. Nurk S, Bankevich A, Antipov D, Gurevich AA, Korobeynikov A, Lapidus A, Prjibelski AD, Pyshkin A, Sirotkin A, Sirotkin Y, Stepanauskas R, Clin-genpeel SR, Woyke T, McLean JS, Lasken R, Tesler G, Alekseyev MA, Pevzner PA. 2013. Assembling single-cell genomes and mini-metagenomes from chimeric MDA products. *J Comput Biol* 20:714–737. <https://doi.org/10.1089/cmb.2013.0084>.
 27. Ozer EA, Allen JP, Hauser AR. 2014. Characterization of the core and accessory genomes of *Pseudomonas aeruginosa* using bioinformatic tools Spine and AGEnt. *BMC Genomics* 15:737. <https://doi.org/10.1186/1471-2164-15-737>.
 28. Bolger AM, Lohse M, Usadel B. 2014. Trimmomatic: a flexible trimmer for Illumina sequence data. *Bioinformatics* 30:2114–2120. <https://doi.org/10.1093/bioinformatics/btu170>.
 29. Richter M, Rossello-Mora R. 2009. Shifting the genomic gold standard for the prokaryotic species definition. *Proc Natl Acad Sci U S A* 106:19126–19131. <https://doi.org/10.1073/pnas.0906412106>.
 30. Larsen MV, Cosentino S, Rasmussen S, Friis C, Hasman H, Marvig RL, Jelsbak L, Sicheritz-Ponten T, Ussery DW, Aarestrup FM, Lund O. 2012. Multilocus sequence typing of total-genome-sequenced bacteria. *J Clin Microbiol* 50:1355–1361. <https://doi.org/10.1128/JCM.06094-11>.
 31. Carrigo JA, Silva-Costa C, Melo-Cristino J, Pinto FR, de Lencastre H, Almeida JS, Ramirez M. 2006. Illustration of a common framework for relating multiple typing methods by application to macrolide-resistant *Streptococcus pyogenes*. *J Clin Microbiol* 44:2524–2532. <https://doi.org/10.1128/JCM.02536-05>.
 32. Schürch AC, Arredondo-Alonso S, Willems RJL, Goering RV. 2018. Whole genome sequencing options for bacterial strain typing and epidemiologic analysis based on single nucleotide polymorphism versus gene-by-gene-based approaches. *Clin Microbiol Infect* 24:350–354. <https://doi.org/10.1016/j.cmi.2017.12.016>.
 33. Long SW, Linson SE, Ojeda Saavedra M, Cantu C, Davis JJ, Brettin T, Olsen RJ. 2017. Whole-genome sequencing of human clinical *Klebsiella pneumoniae* isolates reveals misidentification and misunderstandings of *Klebsiella pneumoniae*, *Klebsiella variicola*, and *Klebsiella quasipneumoniae*. *mSphere* 2:e00290-17. <https://doi.org/10.1128/mSphereDirect.00290-17>.
 34. Fagerquist CK, Bates AH, Heath S, King BC, Garbus BR, Harden LA, Miller WG. 2006. Sub-speciating *Campylobacter jejuni* by proteomic analysis of its protein biomarkers and their post-translational modifications. *J Proteome Res* 5:2527–2538. <https://doi.org/10.1021/pr050485w>.
 35. Fagerquist CK, Garbus BR, Miller WG, Williams KE, Yee E, Bates AH, Boyle S, Harden LA, Cooley MB, Mandrell RE. 2010. Rapid identification of protein biomarkers of *Escherichia coli* O157:H7 by matrix-assisted laser desorption ionization–time-of-flight–time-of-flight mass spectrometry and top-down proteomics. *Anal Chem* 82:2717–2725. <https://doi.org/10.1021/ac902455d>.
 36. Stamm I, Hailer M, Depner B, Kopp PA, Rau J. 2013. *Yersinia enterocolitica* in diagnostic fecal samples from European dogs and cats: identification by Fourier transform infrared spectroscopy and matrix-assisted laser desorption ionization–time of flight mass spectrometry. *J Clin Microbiol* 51:887–893. <https://doi.org/10.1128/JCM.02506-12>.
 37. Dieckmann R, Hammerl JA, Hahmann H, Wicke A, Kleta S, Dabrowski PW, Nitsche A, Stämmler M, Al Dahouk S, Lasch P. 2016. Rapid characterisation of *Klebsiella oxytoca* isolates from contaminated liquid hand soap using mass spectrometry, FTIR and Raman spectroscopy. *Faraday Discuss* 187:353–375. <https://doi.org/10.1039/C5FD00165J>.
 38. Hansen DS, Mestre F, Alberti S, Hernandez-Alles S, Alvarez D, Domenech-Sanchez A, Gil J, Merino S, Tomas JM, Benedi VJ. 1999. *Klebsiella pneumoniae* lipopolysaccharide O typing: revision of prototype strains and O-group distribution among clinical isolates from different sources and countries. *J Clin Microbiol* 37:56–62.
 39. Wyres KL, Wick RR, Gorrie C, Jenney A, Follador R, Thomson NR, Holt KE. 2016. Identification of *Klebsiella* capsule synthesis loci from whole genome data. *Microb Genom* 2:e000102. <https://doi.org/10.1099/mgen.0.000102>.
 40. Rodrigues C, Novais A, Sousa C, Ramos H, Coque TM, Canton R, Lopes JA, Peixe L. 2017. Elucidating constraints for differentiation of major human *Klebsiella pneumoniae* clones using MALDI-TOF MS. *Eur J Clin Microbiol Infect Dis* 36:379–386. <https://doi.org/10.1007/s10096-016-2812-8>.
 41. Christner M, Trusch M, Rohde H, Kwiatkowski M, Schluter H, Wolters M, Aepfelbacher M, Hentschke M. 2014. Rapid MALDI-TOF mass spectrometry strain typing during a large outbreak of Shiga-toxicogenic *Escherichia coli*. *PLoS One* 9:e101924. <https://doi.org/10.1371/journal.pone.0101924>.
 42. Sauget M, Nicolas-Chanoine MH, Cabrolier N, Bertrand X, Hocquet D. 2014. Matrix-assisted laser desorption ionization–time of flight mass spectrometry assigns *Escherichia coli* to the phylogroups A, B1, B2 and D. *Int J Med Microbiol* 304:977–983. <https://doi.org/10.1016/j.ijmm.2014.06.004>.
 43. Holland RD, Duffy CR, Rafi F, Sutherland JB, Heinze TM, Holder CL, Voorhees KJ, Lay JO, Jr. 1999. Identification of bacterial proteins observed in MALDI TOF mass spectra from whole cells. *Anal Chem* 71:3226–3230. <https://doi.org/10.1021/ac990175v>.
 44. Veenemans J, Welker M, van Belkum A, Saccomani MC, Girard V, Pettersson A, Verhulst C, Kluytmans-Vandenberg M, Kluytmans J. 2016. Comparison of MALDI-TOF MS and AFLP for strain typing of ESBL-producing *Escherichia coli*. *Eur J Clin Microbiol Infect Dis* 35:829–838. <https://doi.org/10.1007/s10096-016-2604-1>.
 45. Lau AF, Wang H, Weingarten RA, Drake SK, Suffredini AF, Garfield MK, Chen Y, Gucek M, Youn JH, Stock F, Tso H, DeLeo J, Cimino JJ, Frank KM, Dekker JP. 2014. A rapid matrix-assisted laser desorption ionization–time of flight mass spectrometry-based method for single-plasmid tracking in an outbreak of carbapenem-resistant Enterobacteriaceae. *J Clin Microbiol* 52:2804–2812. <https://doi.org/10.1128/JCM.00694-14>.
 46. Youn JH, Drake SK, Weingarten RA, Frank KM, Dekker JP, Lau AF. 2016. Clinical performance of a matrix-assisted laser desorption ionization–time of flight mass spectrometry method for detection of certain bla_{KPC}-containing plasmids. *J Clin Microbiol* 54:35–42. <https://doi.org/10.1128/JCM.01643-15>.
 47. Sakarikou C, Ciotti M, Dolfa C, Angeletti S, Favalli C. 2017. Rapid detection of carbapenemase-producing *Klebsiella pneumoniae* strains derived from blood cultures by matrix-assisted laser desorption ionization–time of flight mass spectrometry (MALDI-TOF MS). *BMC Microbiol* 17:54. <https://doi.org/10.1186/s12866-017-0952-3>.